Special Feature: Nondestructive Testing and Evaluation Technology

Research Report

Moiré Deflectometry for Measuring Specular Surface Shapes

Tomohiro Hirose

Report received on Nov. 4, 2013

ABSTRACT Moiré deflectometry for measuring 3D specular surface profiles is presented in this paper. In this method, moiré phenomena produced by two pairs of Ronchi gratings are utilized to measure the normal vector distribution of a surface under examination. Unlike conventional deflectometric measurement systems that require complicated calibration, the proposed system only requires simple camera calibration. Surface profiles of deeply curved mirrors with curvature from –20 to 20 m^{-1} were successfully measured using the proposed system. Moreover, part of a miniature vehicle body, which has a complex curved specular surface, was also measured. Furthermore, it was confirmed that the system allows measurement of a normal vector with an angular variation of 0.05 deg.

KEYWORDS Moiré, Deflectometry, Moiré Deflectometry, 3D Shape Measurement, Specular Surface, Phase Measuring Deflectometry

1. Introduction

Optical 3D profilers, which are capable of fast nondestructive acquisition of three-dimensional profiles of physical objects, are becoming indispensable for preparing CAD data of manufactured products and for automatically detecting flaws on the surfaces of objects. There are a lot of optical methodologies for optical 3D profilers such as laser triangulation,[1] fringe projection,[2] white light interferometry,[3,4] classical interferometry,[5,6] and deflectometry.[7-18] It is known that the effectiveness of an optical 3D profiler is restricted by the surface texture of the object under examination.[19] Especially, it is difficult to measure specular objects with widely used triangulation-based methods such as laser triangulation and fringe projection. This fact is an important issue from the viewpoint of a car production because a variety of specular products are used in a car such as body panels, window panes and bumpers. Therefore, 3D optical profilers for specular objects are highly desired.

Among the existing optical measurement methods, interferometry[3-5] and deflectometry[7-18] are applicable to the measurement of specular objects. Particularly, interferometric sensors are capable of measuring specular surfaces with high-precision. However, since the sensors should be configured to probe the object at normal incidence,[4] measurements of objects with deeply curved surfaces and complex shapes are time-consuming. On the other hand, deflectometric sensors are now approaching the accuracy of interferometry due to their extreme sensitivity to gradient changes of a specular reflecting surface.[8,9] Deflectometric measurements are performed with a computer-vision based system that consists of charge coupled device (CCD) cameras and a liquid crystal display (LCD), which allows the measurement of a wide area of curved specular objects. Calibration, which means obtaining the position relationships of pixels in the LCD and CCD cameras in the world coordinate system, is the key to improving the accuracy of the deflectometric system.[8-10] Conventionally, one requires multi-step calibration to obtain the calibration parameters of the deflectometric system. However, this calibration is complicated and is even the cause of systematic errors. Therefore, it is important to reduce the complexity of the calibration procedures for deflectometry to a level similar to that of the triangulation-based method.

Moiré deflectometry,[20-22] which has been studied for several decades, attracts attention as a powerful tool for nondestructive optical testing. O. Kafri et al. first reported a method using moiré deflectometry for measuring the curvature of a specular surface.[20] In this method, the object under examination is placed in the path of a collimated laser beam followed by a pair of transmission gratings located at a certain distance

from each other. Although this method is also applicable to measuring specular surfaces, the measurement systems proposed in the past could only measure a narrow area because of the low numerical aperture of the collimated laser beam. Therefore, it has been difficult to apply this to the measurement of objects with a complex shape.

In this paper, moiré deflectometry with a computer-vision system that consists of CCD cameras, Ronchi gratings and white light illumination for measuring the 3D profile of specular surfaces is presented. Unlike other deflectometric measurement systems that require complicated calibration, the moiré deflectometry proposed here only requires simple camera calibration. Moreover, unlike the past moiré deflectometric system, it has the potential for application to the measurement of deeply curved objects because the proposed system has a high numerical aperture due to the utilization of a white light source, not a collimated laser beam, and cameras.

2. Principle of Moiré Deflectometry

A schematic diagram of moiré deflectometry is shown in **Fig. 1**. Two transmission gratings G_1 and G_2 are placed in front of the white light optical source. The superposition of the gratings produces a moiré fringe. The moiré fringe is reflected by the specular surface of the object being measured, then captured by the CCD camera. The camera lens in this system is focused on the surface under examination. Accordingly, the observed moiré fringe is defocused because it is generated at distance from the surface.

When grating G_1 is moved along the axis perpendicular to the grating plane, the spatial frequency of the moiré fringe is modulated. From the viewpoint of pixel p_1 of the CCD camera, the intensity of the incoming light oscillates as a function of the position ξ of grating G_1. The intensity I is expressed as

$$I(\xi) = \int_{-\gamma/2}^{\gamma/2} I_0 \cdot \cos\left(\frac{2\pi \cdot \tan(\phi+\gamma)\cdot\xi}{\Lambda}\right) d\gamma \,, \quad \cdots\cdots (1)$$

where I_0 is the magnitude of the intensity, ξ is the distance of grating G_1 from the fixed position of grating G_2, γ is the aperture angle of the camera, Λ is the grating pitch, and ϕ is the angle between the movement axis of the grating and the optical axis of the emitted light from the white light source toward the reflection point x_r. Note that Eq. (1) ignores the vertical displacement of the intensity oscillation of the incoming light into pixel p_1. Assuming that ϕ is sufficiently larger than γ, and γ is nearly zero, $\tan(\phi+\gamma)$ is approximated to be $\tan(\phi) + \gamma$. Consequently, $I(\xi)$ can be written as

$$I(\xi) = I_0 \cdot \cos\left(-\frac{2\pi \cdot \tan(\phi)\cdot\xi}{\Lambda}\right) \cdot \frac{\sin(\pi\cdot\gamma\cdot\xi/\Lambda)}{\pi\cdot\xi/\Lambda}. \quad \cdots\cdots\cdots\cdots (2)$$

A schematic diagram of the intensity function $I(\xi)$ is shown in **Fig. 2**. The vertical axis shows the oscillating intensity $I(\xi)$. The horizontal axis shows the position

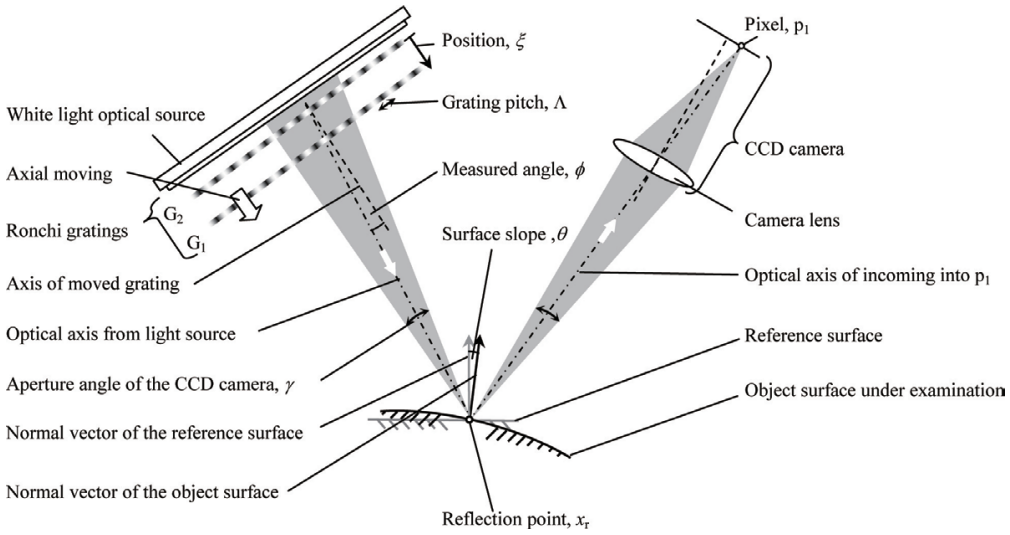

Fig. 1 Schematic diagram of the moiré deflectometry under incoherent illumination.

of grating G_1 with respect to G_2. Note that the wavelength of the oscillation is $\Lambda/\tan(\phi)$, and the envelope of the intensity oscillation indicates a minimum at the position $\xi = \Lambda/\gamma$.

Since the normal vector distribution of the object surface is acquired by measuring the surface slope θ, a plane mirror is required as a reference surface in addition to the object surface. The surface slope θ is calculated using the relation $\theta = (\phi_{obj} - \phi_{ref})/2$, where ϕ_{ref} and ϕ_{obj} are the measured angles for the reference surface and the object surface, respectively. A surface profile of the object is reconstructed by an integration computation of the measured normal vector distribution on the object surface under examination.

In the moiré deflectometry proposed here, the distribution of angle ϕ, which is a ray deflection map of the emitted light from the source, is measured by obtaining the intensity oscillation $I(\xi)$. The intensity oscillation depends only on the distance between the moving grating G_1 and the fixed grating G_2. Therefore, it is possible to place the grating pair G_1-G_2 in any position as long as the moiré reflection is observable with the CCD camera. It is noted that knowledge of the coordinates of the grating pair in the world coordinate system is not required. Consequently, this method only requires camera calibration.

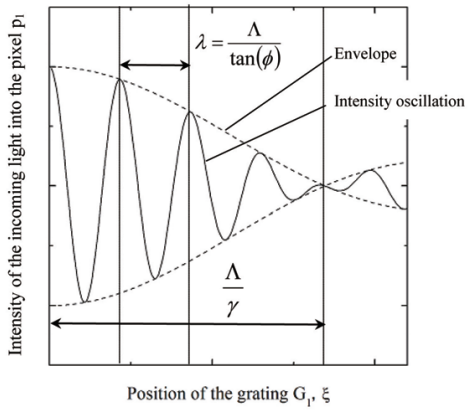

Fig. 2 Intensity of the incoming light into pixel p_1.

3. Measurement System

A schematic diagram of the proposed measurement system is shown in **Fig. 3**. White light illumination of 5,000 K color temperature (Metaphase technologies LED) was used as a light source. A pair of CCD cameras (Basler ace-series A640-100gm/gc) was used as a stereo camera, and was treated as a pair of pinhole cameras in the world coordinate system.

When the surface profile of an object is written as $z = f(x, y)$, the normal vector **n** is expressed as

$$\mathbf{n} = \left[\frac{\partial f}{\partial x}, \quad \frac{\partial f}{\partial y}, \quad 1 \right] \cdots\cdots\cdots\cdots\cdots\cdots (3)$$

In this manner, since the surface slope is represented by two orthogonal components, orthogonally directed gratings are required to detect slope variations. Thus, two pairs of gratings orientated vertically and horizontally were used. The gratings (Howa Sangyo Co. Ltd.) had a grating period of 169 μm and a size of 260×150 mm^2. The grating pairs were placed so that the grating directions were orthogonal to each other. The intermediate gratings, G_2 and G_3, were placed on a scanning stage (Sigma Koki, SGSP20-20) to carry out scanning along the axis perpendicular to the grating plane. Axial movements of the intermediate grating pair G_2 and G_3 were made for 22 mm with 0.05 mm

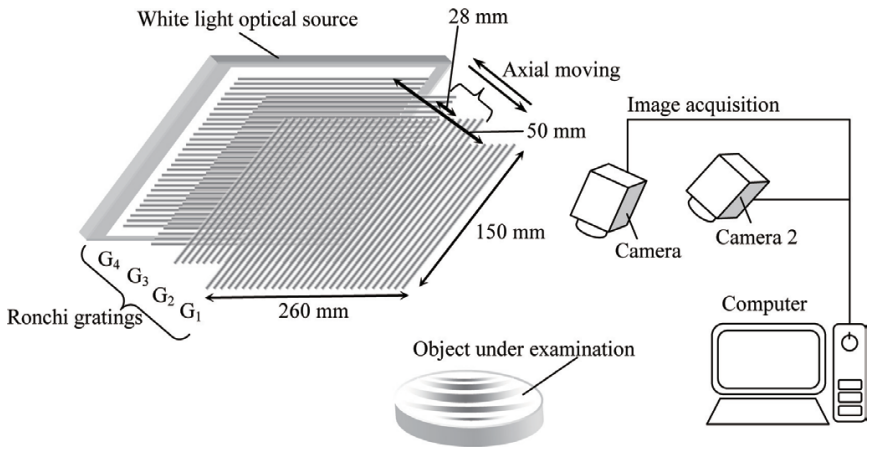

Fig. 3 Schematic diagram of the measurement system.

steps. The intensity oscillation of the incoming light at a certain pixel of a CCD camera is written as a function of the axial distance of grating G_2 from the fixed position of G_1 as

$$I(\xi) = I_{vert}(\xi) + I_{horiz}(\xi - d_{1-4} + d_{2-3}), \cdots\cdots (4)$$

where ξ is the distance of grating G_2 from the fixed position of grating G_1, $I_{vert}(\xi)$ is the intensity oscillation with the vertically directed grating pair G_1-G_2, $I_{horiz}(\xi - d_{1-4} + d_{2-3})$ is the intensity oscillation with the horizontally directed grating pair G_3-G_4, d_{1-4} is the distance between gratings G_1 and G_4, and d_{2-3} is the distance between gratings G_2 and G_3. **Figure 4** indicates an estimation of the intensity oscillation $I(\xi)$ calculated with the parameters of Λ = 169 μm, $\gamma = 57 \times 10^{-3}$ deg, ϕ_{vert} = 8 deg and ϕ_{horiz} = 1 0 deg,

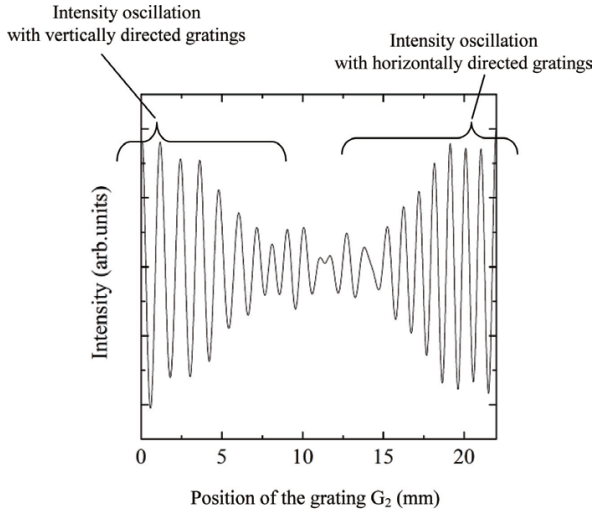

Fig. 4 Estimated intensity oscillation obtained by the proposed system.

where ϕ_{vert} is the angle between the movement axis of the vertical gratings and the optical axis from the light source to the reflection point x_r, and ϕ_{horiz} is the angle between the movement axis of the horizontal gratings and the optical axis. The horizontal axis in Fig. 4 shows the relative position of G_2 to G_1. The vertical axis shows the amplitude of the intensity oscillation observed by the pixel in a CCD camera. It is shown that the magnitude of the intensity gradually decreased as the distance to G_2 increased from 0 to 7 mm, due to the contribution of the vertical grating pair. On the other hand, the magnitude of the intensity oscillation gradually increased as the distance to G_2 increased from 15 to 22 mm, due to the contribution of the horizontal grating pair. In the intermediate region from 7 to 15 mm, the overlap of the intensity oscillation with both grating pairs is shown. Thus the intensity oscillation obtained as a function of the axial position of G_2 is clearly divided into the orthogonal components. Consequently, both azimuths of the normal vector can be easily determined. Additionally, the intermediate grating pair is made to reciprocate motion along the movement axis. The grating pair was shifted 40 μm in both the horizontal and vertical direction parallel to the grating plane before backward scanning to yield an additional intensity oscillation measurement with a π/2 phase shift. The angular variation of the normal vector was obtained by analyzing the intensity oscillations with and without shifted phase.

Figure 5(a) shows a schematic diagram of the stereo camera system used in the proposed method. Cameras 1 and 2 capture two different views of the moiré reflection on the surface under examination. Stereo matching, which finds a pixel p_2 in Camera 2 that

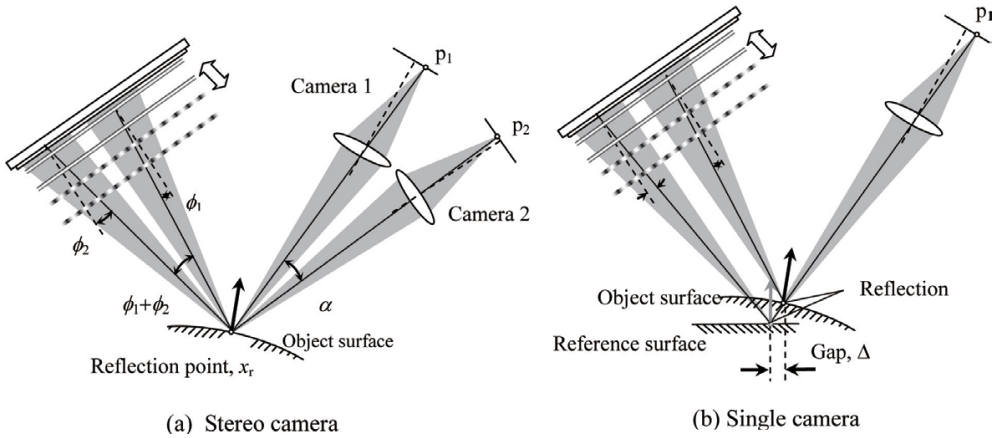

Fig. 5 Schematic diagram of the proposed system.

corresponds to a specific pixel p_1 in Camera 1, is carried out to obtain the coordinates of the reflection point x_r in the world coordinate system. The stereo matching algorithm is based on the fact that the angle α is equal to $\phi_1 + \phi_2$, where α is the angle between the axes of the incoming light into pixels p_1 and p_2, and ϕ_1 and ϕ_2 are the angles between the movement axis of the grating and the optical axes from the light source which are the optical axes of the incoming light into pixels p_1 and p_2, respectively. The angle α is obtained as a result of the stereo camera calibration, and $\phi_1 + \phi_2$ is obtained as a result of the analyses of the intensity function generated by the moving gratings. The single camera system shown in Fig. 5(b) could not function using the proposed method because the coordinates of the reflection point of the object are not always coincident with those of the reference surface. A gap Δ between the coordinates of the reflection positions of the reference surface and that of the object surface is apparent from the inspection of pixel p_1, where lights reflected by the reference and the object surfaces are incoming. The gap Δ causes an error in the position of the normal vector of the object surface under examination. If a deeply curved surface is measured, the error associated with Δ could be particularly significant.

For the experiment, the surface profiles of nine mirrors with curvatures from –20 to 20 m^{-1} (Sigma Koki) were measured using the proposed measurement system. In addition, a miniature vehicle body (StarTech Service, Inc., STI Mini-D), called the "speed shape", was also measured to demonstrate a possible application of the proposed system. A picture of the "speed shape" is shown in **Fig. 6**. Its surface was plated with Cr to make it specular. The "speed shape" has a length of 200 mm, a width of 90 mm and a height of 50 mm.

4. Experimental Results

Figure 7(a) shows pictures of the moiré reflection on a convex mirror. The direction of the moiré fringe varies continuously from vertical to horizontal as a function of the position of grating G_2. The intensity oscillation at a specific pixel is shown in Fig. 7(b). As expected, both of the contributions due to the vertically and horizontally directed grating pairs are observed in the intensity oscillation.

Figure 8(a) indicates the typical surface profile of a convex mirror. The surface profile was integrated from the normal vector distribution measured using the proposed system using a computation proposed by S. Ettl et al.[23] It is shown that the surface profile was successfully reconstructed from the normal vector distribution measured by the proposed system. Then the curvatures of the reconstructed surface profiles of the examined mirrors were evaluated. Figure 8(b)

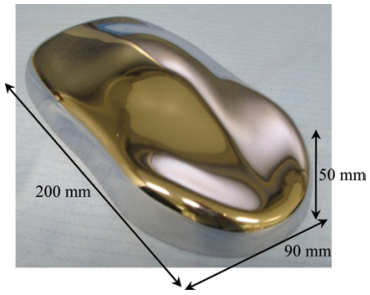

Fig. 6 Cr-plated miniature vehicle body "speed shape".

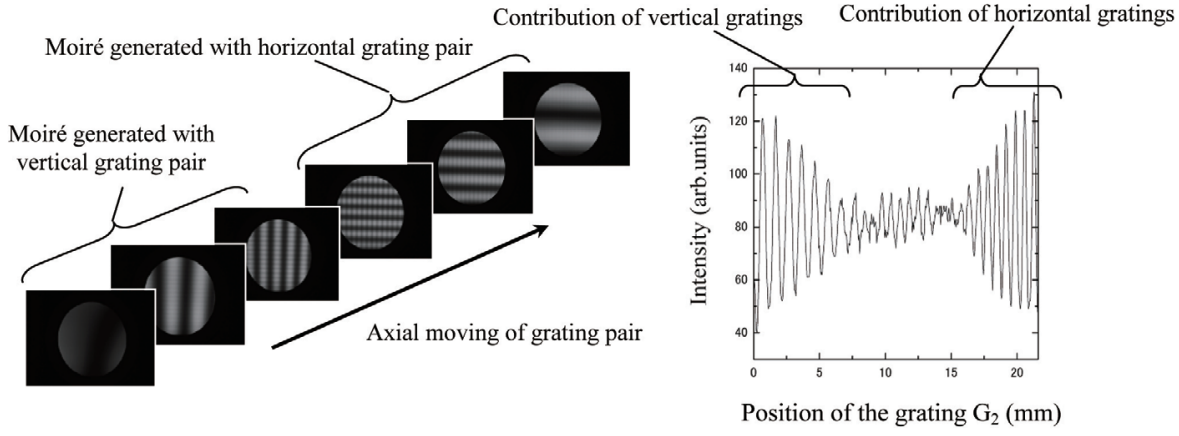

(a) Moiré reflected by a convex (b) Intensity oscillation observed at a specific

Fig. 7 Moiré reflection observed on a convex mirror under examination.

indicates the estimated curvatures of the examined mirrors. Through linear regression analysis, the relationship between the estimated and the actual curvatures was determined to be

$$\kappa_E = (1.11 \pm 0.03) \cdot \kappa_A + (0.02 \pm 0.21), \quad \cdots\cdots\cdots (5)$$

where κ_E is the estimated curvature and κ_A is the actual curvature of the examined mirrors. It is shown that the estimated curvatures of the reconstructed surface profiles measured by the proposed method are in good agreement with the actual curvatures of the examined mirrors.

Figure 9 shows the reconstructed surface profile of the "speed shape" measured by the proposed system. As can be seen from the figure, the measured part of the "speed shape" was reasonably well reconstructed, although a more quantitative investigation such as a comparison between the 3D profile obtained with the proposed system and that obtained using other equipment is needed.

5. Discussion

The detection limit of the measurable angular variation with the proposed system is estimated in this discussion. A plane mirror tilted with an angular variation of $\Delta\theta$ is considered. In this case the variation of the intensity oscillation ΔI measured with the proposed system can be expressed as

$$\Delta I = I_0 \cdot \frac{\sin(\pi \cdot \gamma \cdot \xi / \Lambda)}{\pi \cdot \xi / \Lambda} \cdot \left\{ \cos\left(-\frac{2\pi \cdot \tan(\varphi + \Delta\theta) \cdot \xi}{\Lambda} \right) - \cos\left(-\frac{2\pi \cdot \tan(\varphi) \cdot \xi}{\Lambda} \right) \right\}. \quad \cdots\cdots\cdots\cdots (6)$$

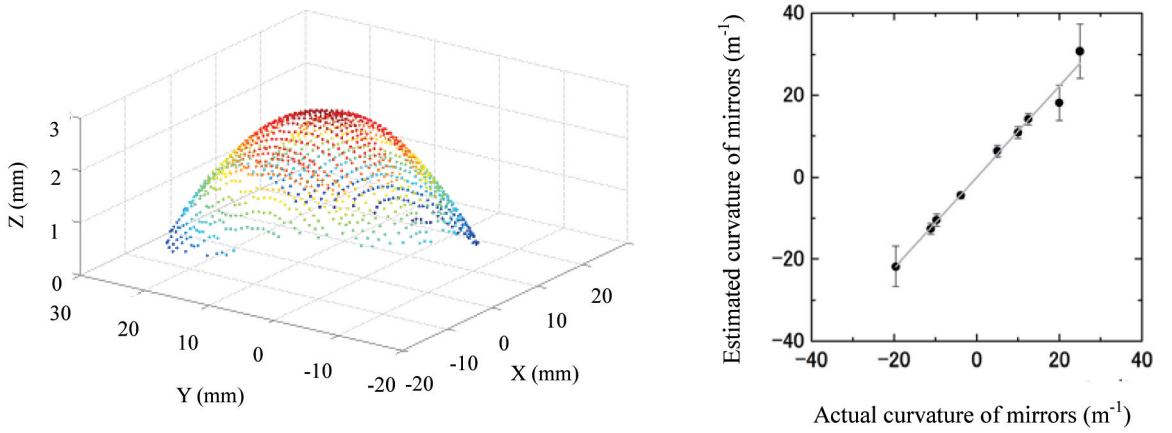

(a) Reconstructed surface profile of a convex mirror (b) Estimated curvature of nine mirrors

Fig. 8 Experimental results for the mirrors.

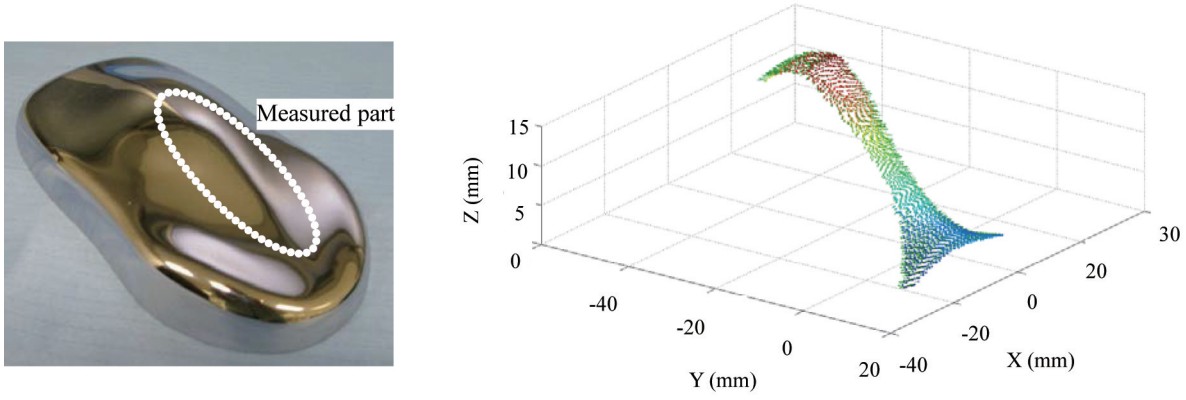

Fig. 9 Reconstructed surface profile of part of the "speed shape".

Assuming that $\Delta\theta$ is nearly zero, $\tan(\phi + \Delta\theta)$ is approximated to be $\tan(\phi) + \Delta\theta$. Accordingly, ΔI is rewritten as

$$\Delta I = I_0 \cdot \frac{\sin(\pi \cdot \gamma \cdot \xi / \Lambda)}{\pi \cdot \xi / \Lambda} \cdot \left\{ \cos\left(-\frac{2\pi \cdot (\tan(\varphi) + \Delta\theta) \cdot \xi}{\Lambda} \right) - \cos\left(-\frac{2\pi \cdot \tan(\varphi) \cdot \xi}{\Lambda} \right) \right\}. \quad \cdots\cdots\cdots\cdots (7)$$

By utilizing trigonometric functions, Eq. (7) can be expressed as follows:

$$\begin{aligned} \Delta I &= -2 \cdot I_0 \cdot \frac{\sin(\pi \cdot \gamma \cdot \xi / \Lambda)}{\pi \cdot \xi / \Lambda} \cdot \sin\left(-\frac{\pi \cdot \Delta\theta \cdot \xi}{\Lambda} \right) \cdot \sin\left(-\frac{\pi \cdot \xi \cdot (2\tan(\varphi) + \Delta\theta)}{\Lambda} \right) \\ &= -2 \cdot I_0 \cdot \frac{\sin(\pi \cdot \gamma \cdot \xi / \Lambda)}{\pi \cdot \xi / \Lambda} \cdot \sin\left(-\frac{\pi \cdot \Delta\theta \cdot \xi}{\Lambda} \right) \\ &\quad \cdot \left[\sin\left(-\frac{2\pi \cdot \xi \cdot \tan(\varphi)}{\Lambda} \right) \cdot \cos\left(-\frac{\pi \cdot \xi \cdot \Delta\theta}{\Lambda} \right) - \cos\left(-\frac{2\pi \cdot \xi \cdot \tan(\varphi)}{\Lambda} \right) \cdot \sin\left(-\frac{\pi \cdot \xi \cdot \Delta\theta}{\Lambda} \right) \right]. \end{aligned} \quad \cdots\cdots\cdots (8)$$

If a variable, β, is small enough, $\sin(\beta)$, $\cos(\beta)$ and β^2 are approximated to be β, 1 and 0, respectively. Therefore, the following relationship is obtained.

$$\Delta I = 2I_0 \cdot \sin\left(\frac{\pi \cdot \gamma \cdot \xi}{\Lambda} \right) \cdot \sin\left(-\frac{2\pi \cdot \xi \cdot \tan(\phi)}{\Lambda} \right) \cdot \Delta\theta \quad \cdots\cdots\cdots\cdots\cdots (9)$$

Equation (9) indicates that the angular variation $\Delta\theta$ is measurable if the magnitude of ΔI is larger than the noise intensity I_N. This condition is expressed by the following relationships.

$$\begin{cases} I_N \le 2I_0 \cdot \Delta\theta \cdot \sin\left(\dfrac{\pi \cdot \gamma \cdot \xi}{\Lambda} \right) & \text{if } \xi < \dfrac{\Lambda}{2\gamma} \\ I_N \le 2I_0 \cdot \Delta\theta & \text{if } \xi \ge \dfrac{\Lambda}{2\gamma} \end{cases} \quad \cdots\cdots (10)$$

Here the scanning length ξ is assumed to be sufficiently long, i.e., $\xi > \Lambda/2\gamma$. In addition, it is possible to increase I_0 to the maximal camera response V_{max} of the CCD cameras. If the noise intensity I_N is only due to the noise in the CCD camera system, I_N is replaced with V_N which is the noise of the CCD camera. Then the relationship between the noise V_N and the angular variation $\Delta\theta$ can be written simply as

$$\Delta\theta \ge \frac{V_N}{2 \cdot V_{max}}. \quad \cdots\cdots\cdots\cdots\cdots\cdots (11)$$

Equation (11), using the expression of "dynamic range", R, is rewritten as follows:

$$\Delta\theta \ge \frac{1}{2 \cdot 10^{R/20}}, \quad \cdots\cdots\cdots\cdots\cdots\cdots (12)$$

where $R = -20 \log(V_N/V_{max})$. Note that $\Delta\theta$ is independent of the grating pitch Λ and the aperture angle γ if the scanning length is longer than $\Lambda/2\gamma$. The dynamic range R is generally 50-60 dB in a CCD camera; thus, $\Delta\theta$ is estimated to be 0.1-0.05 deg.

To confirm this estimation experimentally, the normal vector distribution of a plane mirror tilted from 0 to 1 deg was measured. **Figure 10** shows the experimental results. The vertical and horizontal axes show the estimated angular variation measured using the proposed system and the actual angular variation of the examined mirrors, respectively. The error bar of each point indicates the standard deviation calculated from the normal vector distribution in an area of 30 × 30 mm^2 on the measured plane mirror. The average of the standard deviations over the whole plot is 0.05 deg. This value is almost in agreement with the estimation using Eq. (12). Consequently, it has been verified that the proposed system can measure the normal vector of an object surface with an angular variation of 0.05 deg.

6. Conclusion

Moiré deflectometry with a computer-vision system, utilizing a white light source, Ronchi gratings and CCD cameras, for measuring the 3D shape of a

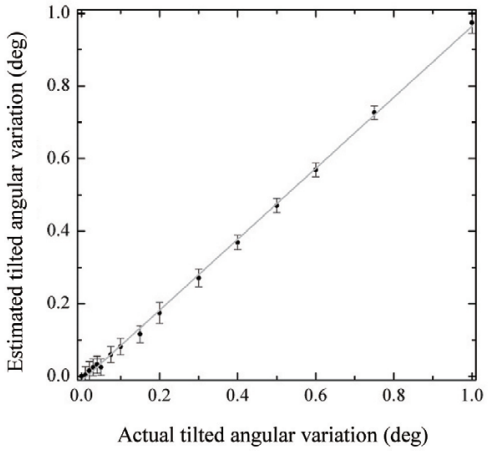

Fig. 10 Comparison between the estimated and the actual angles of the tilted plane mirror.

specular surface has been presented. The moiré fringe is reflected by a specular object, and observed by a calibrated stereo camera. The proposed system only requires camera calibration. Therefore, it has the potential to be developed into a 3D profiler for complex specular surfaces. In the experiment, deeply curved mirrors with curvature from –20 to 20 m^{-1} were successfully measured. Moreover, part of a miniature vehicle body with a complex curved specular surface was also measured. Furthermore, the proposed system allows measurement of a normal vector with an angular variation of 0.05 deg.

Acknowledgement

This paper is based on the original publication of SPIE by Tomohiro Hirose and Tsunaji Kitayama, entitled "Moiré deflectometry under incoherent illumination: 3D profiler for specular surfaces", Proc. of SPIE Vol. 8788 (2013), 87881G.

References

(1) Dorsch, R. G., Häusler, G. and Herrmann, J. M., "Laser Triangulation: Fundamental Uncertainty in Distance Measurement", *Appl. Opt.*, Vol. 33, No. 7 (1994), pp. 1306-1314.
(2) Malacala, D., *Optical Shop Testing* (2007), pp. 756-809, Wiley-Interscience.
(3) Dresel, T., Häusler, G. and Venzke, H., "Three-dimensional Sensing of Rough Surfaces by Coherence Radar", *Appl. Opt.*, Vol. 31, No. 7 (1992), pp. 919-925.
(4) Leach, R., Optical *Measurement of Surface Topography* (2011), pp. 187-206, Springer.
(5) Wagner, J. W. and Spicer, J. B., "Theoretical Noise-limited Sensitivity of Classical Interferometry", *J. Opt. Soc. Am. B*, Vol. 4, No. 8 (1987), pp. 1316-1326.
(6) Leach, R., *Optical Measurement of Surface Topography* (2011), pp. 167-185, Springer.
(7) Knauer, M. C., Kaminski, J. and Häusler, G., "Phase Measuring Deflectometry: A New Approach to Measure Specular Free-form Surfaces", *Proc. of SPIE*, Vol. 5457 (2004), pp. 366-376.
(8) Faber, C., Olesch, E., Roman, K. and Häusler, G., "Deflectometry Challenges Interferometry: The Competition Gets Tougher!", *Proc. of SPIE*, Vol. 8493 (2012), 84930R.
(9) Häusler, G., Faber, C., Olesch, E. and Ettl, S., "Deflectometry vs. Interferometry", *Proc. of SPIE*, Vol. 8788 (2013), 87881C.
(10) Su, P., Khreishi, M., Huang, R., Su, T. and Burge, J. H., "Precision Aspheric Optics Testing with SCOTS: A Deflectometry Approach", *Proc. of SPIE*, Vol. 8788 (2013), 87881E.
(11) Su, P., Parks, R. E., Wang, L., Angel, R. P. and Burge, J. H., "Software Configurable Optical Test System: A Computerized Reverse Hartmann Test", *Appl. Opt.*, Vol. 49, No. 23 (2010), pp. 4404-4412.
(12) Pak, A., "Reconstruction of Specular Surface via Probabilistic Voxel Carving", *Proc. SPIE*, Vol. 8791 (2013), 87911B.
(13) Balzer, J. and Werling, S., "Principle of Shape from Specular Reflection", *Measurement*, Vol. 43, No. 10 (2010), pp. 1305-1317.
(14) Skydan, O. A., Lalor, M. J. and Burton, D. R., "3D Shape Measurement of Automotive Glass by Using a Fringe Reflection Technique", *Meas. Sci. Technol.*, Vol. 18, No. 1 (2007), pp. 106-114.
(15) Werling, S., Mai, M., Heizmann, M. and Beyerer, J., "Inspection of Specular and Partially Specular Surfaces", *Metrol. Meas. Syst.*, Vol. 16, No. 3 (2009), pp. 415-431.
(16) Tang, Y., Su, X., Wu, F. and Liu, Y., "A Novel Phase Measuring Deflectometry for Aspheric Mirror Test", *Optics Express*, Vol. 17, No. 22 (2009), pp. 19778-19784.
(17) Huang, L., Ng, C. S. and Asundi, A. K., "Dynamic Three-dimensional Sensing for Specular Surface with Monoscopic Fringe Reflectometry", *Optics Express*, Vol. 19, No. 13 (2011), pp. 12809-12814.
(18) Hirose, T. and Kitayama, T. "Moiré Deflectometry Under Incoherent Illumination: 3D Profiler for Specular Surfaces", *Proc. of SPIE*, Vol. 8788 (2013), 87881G.
(19) Knauer, M. C., Ritcher, C. and Hausler, G., "3D Sensor Zoo: Species and Natural Habitats", *Laser Technik Journal*, Vol. 3, No. 1 (2006), pp. 33-37.
(20) Kafri, O., "Noncoherent Method for Mapping Phase Objects", *Optics Letters*, Vol. 12, No. 10 (1980), pp. 555-557.
(21) Kafri, O. and Glatt, I., *The Physic of Moiré Metrology* (1990), pp. 89-171, Wiley-Interscience.
(22) Rasouli, S., Dashti, M. and Ramaprakash, A. N., "An Adjustable, High Sensitivity, Wide Dynamic Range Two Channel Wave-front Sensor Based on Moiré Deflectometry", *Optics Express*, Vol. 18, No. 23 (2010), pp. 23906-23915.
(23) Ettl, S., Kaminski, K., Knauer, M., C. and Häusler, G., "Shape Reconstruction from Gradient Data", *Appl. Opt.*, Vol. 47, No. 12 (2008), pp. 2091-2097.

Figs. 3, 5, 6, 7(a) and 9
Reprinted from Proc. of SPIE, Vol. 8788 (2013), 87881G, Tomohiro Hirose and Tsunaji Kitayama, "Moiré Deflectometry under Incoherent Illumination: 3D Profiler for Specular Surfaces", © 2013 SPIE, with permission from SPIE.

Tomohiro Hirose

Research Field:
- Optical Measurement for Nondestructive Testing

Academic Degree: Dr.Eng.
Academic Societies:
- The Japan Society of Applied Physics
- The International Society for Optics and Photonics

